

## ELECTROLESS NICKEL AND COPPER METALLIZATION: CONTACT FORMATION ON CRYSTALLINE SILICON AND BACKGROUND PLATING BEHAVIOR ON PECVD $\text{SiN}_x\text{:H}$ LAYERS

Stefan Braun, Erkan Emre, Bernd Raabe, Giso Hahn

University of Konstanz, Department of Physics, P.O. Box X916, 78457 Konstanz, Germany

Author for correspondence: stefan.braun@uni-konstanz.de, Tel.: +49 7531 882082, Fax: +49 7531 883895

**ABSTRACT:** An alternative approach to the silver thick film metallization for the front side of silicon solar cells can be implemented by electroless nickel and copper deposition. One of the most challenging problems for a wet-chemical metallization sequence using nickel and copper is the phenomenon of background plating. Hereby the metal is not only deposited on the opened emitter structure but also on the insulating PECVD silicon nitride layer which causes additional shading to the solar cell. Contact properties of the metallization like contact resistance, adhesion and line resistance must be optimized. The nickel-silicon contact can be enhanced by an additional sintering step. In this paper the requirements for an adequate nickel silicide formation are discussed and it is shown how to reduce the problem of background plating on PECVD  $\text{SiN}_x\text{:H}$  surfaces.

**Keywords:** Nickel plating, nickel silicide, background plating

### 1 INTRODUCTION

The wet-chemical deposition of metals offers several advantages in contrast to the widespread screen printing technology. A significant reduction of the shading losses results from narrow metal fingers. The deposition temperature of nickel and copper is low and it is not necessary to perform a high temperature step at the end of the metallization. This offers new technological possibilities. For example, it is possible to implement a dielectric rear side passivation which is sensitive to high temperature steps instead of using a screen printed aluminum back surface field. Low temperature contact formation can be included in advanced solar cell concepts.

Nickel is an ideal candidate for wet-chemical deposition, because it serves as diffusion barrier for copper and low contact resistances to doped silicon can be achieved. By forming an alloy of nickel and silicon the contact resistance can be reduced further. This is done by heating the stack system in a nitrogen atmosphere. The formation of three alloys ( $\text{Ni}_2\text{Si}$ ,  $\text{NiSi}$ ,  $\text{NiSi}_2$ ) can be observed at different temperatures 200-350°C, 350-750°C and >750°C [1].

Several nickel plating solutions also contain phosphorus therefore the formation temperature of a nickel silicide layer is also dependent on the phosphorus embedded in the nickel layer.

A completely closed and sintered nickel seed layer provides an excellent contact resistance and also acts as a diffusion barrier for a thick copper layer which provides even higher conductivity for the front side metallization.

It is common for buried contact silicon solar cells to use LPCVD (Low Pressure Chemical Vapor Deposition) silicon nitride and Czochralski (Cz) grown wafer material. Using LPCVD silicon nitride one can avoid the background plating of the deposited metal on the  $\text{SiN}_x$  surface because the LPCVD silicon nitride layer is dense and is known to have a low pinhole density compared to PECVD (Plasma Enhanced Chemical Vapor Deposition) silicon nitride layers. The tips and edges of the texture are completely covered by silicon nitride. On the other hand PECVD silicon nitride ( $\text{SiN}_x\text{:H}$ ) has better bulk and surface passivation capabilities compared to LPCVD silicon nitride [2], because of a higher hydrogen content.

For multicrystalline wafer material with a high amount of defects, it is necessary to use PECVD  $\text{SiN}_x\text{:H}$  for a sufficient bulk passivation [3]. In that case one can only use a single diffusion step, the hydrogen would diffuse out of the wafer during a second high temperature step [4].

The PECVD  $\text{SiN}_x\text{:H}$  should therefore be optimized for a high coverage of the edges and tips of the surface texture. Additionally, a plating technology for PECVD  $\text{SiN}_x\text{:H}$  must be developed which guarantees no background plating, a low contact and line resistance, low shading losses and good adhesions characteristics.

### 2 SAMPLE PREPARATION

Figure 1 shows the complete production sequence of the samples prepared for the experiment. Starting with textured Cz-Si wafers, samples with different  $\text{POCl}_3$  emitters (22  $\Omega/\text{sq}$ , 53  $\Omega/\text{sq}$ , 97  $\Omega/\text{sq}$  and 151  $\Omega/\text{sq}$ ) were prepared. The 151  $\Omega/\text{sq}$  emitter was realized by a shallow 100  $\Omega/\text{sq}$  emitter diffusion, followed by P-glass removal and thermal oxidation.

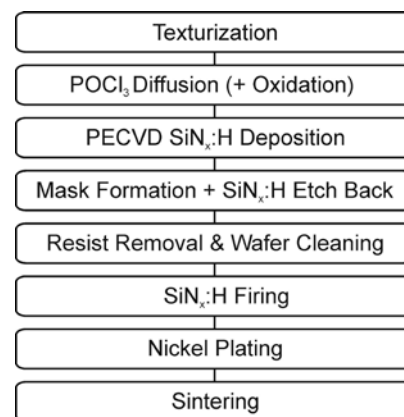


**Figure 1:** Production sequence of the samples used for the wet-chemical metal deposition experiments.

After the emitter diffusion, the P-glass was removed in diluted HF. The wafers were coated with PECVD  $\text{SiN}_x\text{:H}$ . The  $\text{SiN}_x\text{:H}$  surface was coated with etch resist and TLM (Transfer Length Method) structures were

applied by photolithography (mask formation in Figure 1). The contact fingers were 500  $\mu\text{m}$  wide and the distance between the contact fingers was increased by 100  $\mu\text{m}$  for each finger.

The  $\text{SiN}_x\text{:H}$  was etched back in diluted HF. After rinsing the samples in DI water, the resist was removed in Acetone. The samples were rinsed again in DI water and fired in a belt furnace. By firing the samples, the morphology of the  $\text{SiN}_x\text{:H}$  structure changes, the layer gets slightly denser. Photolithography was used to define precise TLM structures. Even small deviations of a few microns for the contact finger structure can cause large fluctuations for the specific contact resistance.

A different approach to produce samples for a wet-chemical process may be the Laser Chemical Processing (LCP) method [5]. Hereby a laser opens the  $\text{SiN}_x\text{:H}$  and forms a selective emitter structure.

### 3 EXPERIMENT

To determine the optimal thickness of the nickel layer, the deposition time of the TLM samples was varied from one to ten minutes. The temperature of the electroless nickel bath was 40°C. Scanning Electron Microscopy (SEM) pictures were taken before and after sintering of the samples. The optimal nickel layer should cover the opened silicon surface completely even after the sintering step because the nickel surface should act as a diffusion barrier.

The results of the plating tests were used to prepare the samples with the TLM structures. Therefore four different emitters were used. The 22  $\Omega/\text{sq}$  emitter represents an emitter which is easy to contact and deep so that shunting of the pn-junction is prevented even at high temperatures. An emitter in the region of 50  $\Omega/\text{sq}$  is often used for industrial-type solar cells in the screen printing process because formation of the front contact is still feasible. The 97  $\Omega/\text{sq}$  emitter is shallow and may be shunted easily. It cannot be contacted by standard screen printing Ag pastes any more. The 151  $\Omega/\text{sq}$  emitter is deep because of an additional oxidation step after the emitter diffusion, but has a very low surface concentration. It is questionable if this kind of emitter can be contacted well. This kind of emitter cannot be used in a screen printing processes.

The samples were electroless plated for 180 seconds at about 40°C and rinsed in DI water afterwards. The samples were sintered at temperatures of 350°C, 400°C, 450°C and 500°C, respectively, for five minutes in a RTP (Rapid Thermal Process) furnace under nitrogen atmosphere. The structures were cut in two millimeter broad strips by a dicing saw. To compare the samples with different emitters and firing parameters the voltage resulting from a given current was measured with TLM and the specific contact resistance was determined [6].

The emitter profiles were measured by ECV (Electrochemical Capacity Voltage) to compare the depth and surface concentration.

Two types of  $\text{SiN}_x\text{:H}$  surfaces were analyzed with an optical microscope under high illumination. Both samples were covered with PECVD  $\text{SiN}_x\text{:H}$ . One sample was cleaned in diluted HCl and diluted HF before deposition. The second sample was cleaned in diluted  $\text{NH}_3 + \text{H}_2\text{O}_2$  followed by a HF dip and an additional diluted HCl +  $\text{H}_2\text{O}_2$  cleaning and HF dip, called RCA

cleaning. Afterwards the sample was coated with silicon nitride.

### 4 RESULTS

It can be observed that after a plating time of 3 minutes the sample is completely covered with nickel. The longer the plating time, the thicker the resulting nickel layer.

A picture of a completely covered nickel seed layer before and after sintering is illustrated in figure 2.

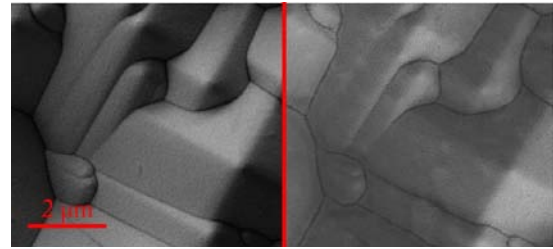


**Figure 2:** On the left side an electroless plated nickel layer is shown. On the right side, the layer is sintered for 5 minutes at 450°C.

Samples which were plated for more than 4 minutes showed inhomogeneities after sintering. It was observed that the nickel layer was partly opened especially on the edges of the pyramids. This may be caused by thermal stress in the metal layer. Figure 3 shows a sample which was plated for 7 minutes and sintered afterwards.

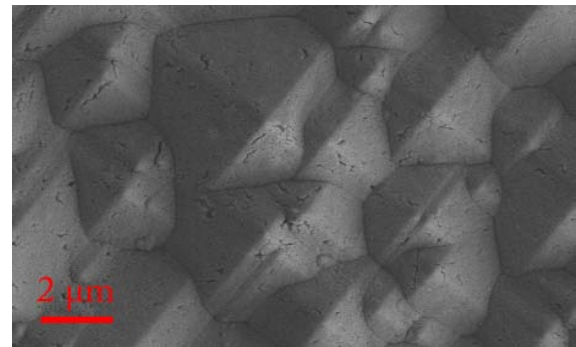


**Figure 3:** Sintered sample with cracks in the nickel layer.

To ensure that the nickel silicide was formed, a sample which was sintered for 5 minutes at 400°C was etched back in diluted  $\text{HNO}_3 + \text{HCl}$  solution and rinsed in DI water afterwards. It is seen that the alloy is not formed as a layer. The alloy has a rough sponge-like structure. This may be a reason why the adhesion of sintered samples is higher compared to non sintered samples. Figure 4 shows the SEM picture of an etched back sample.

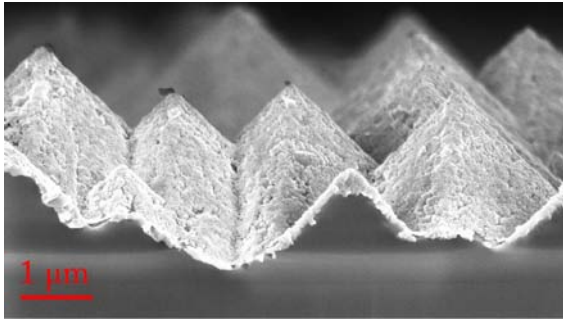


**Figure 4:** Sintered nickel layer etched back in diluted  $\text{HNO}_3 + \text{HCl}$ . The alloy can be seen now.

The emitter profiles were evaluated by ECV measurement to determine the profiles and the surface concentrations of the emitters. Figure 5 shows the emitter profiles of the four TLM test structures.

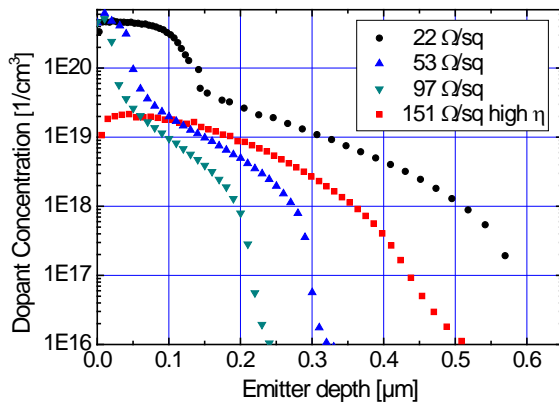


**Figure 5:** Four emitter profiles of the TLM samples measured with ECV method. (Wafer Profiler CVP21, WEP).

Figure 6 shows the graph of the TLM measurement for the 151  $\Omega/\text{sq}$  emitter at four different sintering temperatures. It can be seen that the sheet resistance of the samples varies slightly because the slope of the straight lines varies. This phenomenon is caused by the slightly inhomogeneous emitter diffusion.

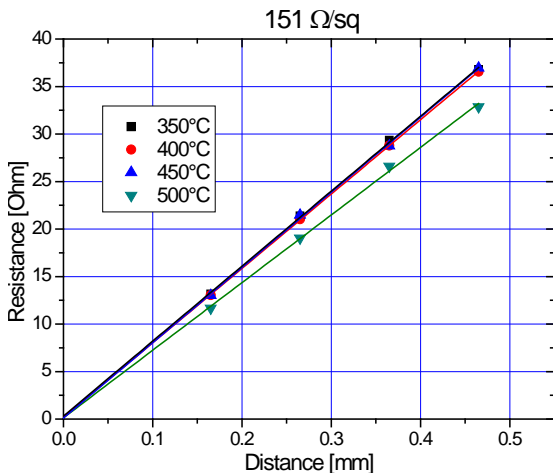


**Figure 6:** TLM graph of the 151  $\Omega/\text{sq}$  emitter for different sintering temperatures.

The specific contact resistance for all emitters at sintering temperatures of 350°C, 400°C, 450°C and 500°C is presented in table I. Samples with titanium, palladium, and silver metallization served as reference. These samples were produced by electron beam evaporation followed by an annealing step at 350°C for 30 minutes in nitrogen atmosphere.

**Table I:** Specific contact resistances for different emitters and sintering temperatures with Ti/Pd/Ag samples as reference. Sheet resistance measured by ECV on one sample.

	Nickel	Nickel	Nickel	Nickel	TiPdAg
$T_{\text{Sinter}}$	350°C	400°C	450°C	500°C	350°C
$R_{\text{Sh}}$ [ $\Omega/\square$ ]	$\rho_c$ [ $\text{m}\Omega\text{cm}^2$ ]	$\rho_c$ [ $\text{m}\Omega\text{cm}^2$ ]	$\rho_c$ [ $\text{m}\Omega\text{cm}^2$ ]	$\rho_c$ [ $\text{m}\Omega\text{cm}^2$ ]	$\rho_c$ [ $\text{m}\Omega\text{cm}^2$ ]
22	0.007	0.033	0.007	0.033	0.010
53	0.121	0.003	0.002	0.04	0.001
97	0.406	0.266	0.363	0.065	---
151	0.143	0.120	0.111	0.100	---

The sheet resistances obtained by ECV-measurement are comparable to the sheet resistances of the TLM-method and presented in table II. This indicates no significant shunting of the junction. The specific contact resistance  $\rho_c$  seems to decrease with higher temperatures and increases with higher sheet resistance.

It should be noted that the TLM measurement is a very sensitive measuring method. If the distance between the contacting fingers is not determined exactly, strong deviations of the specific contact resistance can occur. That is why photolithography was used for the sample preparation. An additional approach by selectively covering the silicon nitride layer by inkjet printing showed no satisfying results.

**Table II:** Sheet resistance measured by ECV and TLM.

	Nickel	Nickel	Nickel	Nickel	TiPdAg
$T_{\text{Sinter}}$	350°C	400°C	450°C	500°C	350°C
$R_{\text{Sh}}$ [ $\Omega/\square$ ]	$R_{\text{Sh}}$ [ $\Omega/\square$ ]	$R_{\text{Sh}}$ [ $\Omega/\square$ ]	$R_{\text{Sh}}$ [ $\Omega/\square$ ]	$R_{\text{Sh}}$ [ $\Omega/\square$ ]	$R_{\text{Sh}}$ [ $\Omega/\square$ ]
ECV	TLM	TLM	TLM	TLM	TLM
22	17.1	18.3	19.3	20.9	19.6
53	44.8	51.3	49.2	49.6	44.7
97	78.1	93.4	89.1	93.9	---
151	157.8	158.0	155.4	143.5	---

This experiment showed that it is possible to contact an emitter structure with an electrically active surface doping level of  $2 \times 10^{19}/\text{cm}^3$  by electroless nickel deposition. Compared to the Ti/Pd/Ag metallization, the specific contact resistance of the sintered nickel metallization is in the same order of magnitude for optimal nickel sintering parameters. The screen printed silver metallization technology is widely used for industrial produced silicon solar cells. The typical specific contact resistances are between 1 to 10  $\text{m}\Omega\text{cm}^2$  [7].

Investigations with an optical microscope are shown in figure 7. The  $\text{SiN}_x\text{:H}$  layers of sample (a) and (b) were deposited with PECVD whereby sample (b) got a RCA

cleaning and sample (a) was cleaned in HCl followed by an HF dip. On sample (a) several bright spots (marked in red) are visible. It can be observed that sample (b) shows no significant inhomogeneities.

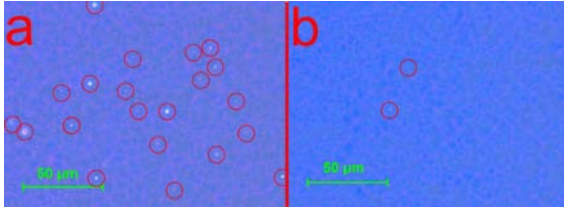


**Figure 7:** a) PECVD sample with HCl cleaning. Red circles indicate impurities. b) PECVD sample with RCA cleaning.

We assume that the bright spots are impurities which can be removed or strongly reduced by the RCA cleaning.

Up to now it is not completely understood if the cleaning process of sample (b) inhibits the background plating completely, but it is assumed and a topic for ongoing research.

## 5 CONCLUSION

A uniform nickel seed layer was electroless deposited on a textured silicon substrate. By adjusting the thickness of the layer, cracking of the nickel layer could be prevented during nickel silicide formation in a RTP furnace. A completely covering nickel layer acting as a diffusion barrier could be reached with only one nickel deposition step.

It was demonstrated that an electroless plated and sintered nickel layer is able to contact emitters from  $20 \Omega/\text{sq}$  to  $151 \Omega/\text{sq}$  with specific contact resistance of  $0.1 \text{ m}\Omega\text{cm}^2$  or below by optimal sintering conditions. By depositing a thin nickel layer, shallow emitters of 250 nm widths indicates no shunting, even at sintering temperatures of  $500^\circ\text{C}$  for 5 minutes. Compared to a screen printed silver metallization, the specific contact resistance of the nickel samples is significantly lower and in the region of a high efficiency metallization realized by Ti/Pd/Ag evaporation. There are hints that an adjusted cleaning sequence can decrease background plating.

## 6 OUTLOOK

Electroless nickel deposition offers a new field for advanced silicon solar cell concepts. It allows contacting emitters with high sheet resistance so it might not be necessary to use a selective emitter structure. In combination with a low temperature wet-chemical metal deposition, for instance silver or copper plating, it is possible to include dielectric rear side passivation schemes like  $\text{Al}_2\text{O}_3$  layers in a low temperature metallization process.

## 9 REFERENCES

- [1] J.W. Mayer, S.S. Lau, *Electronic Materials Science: For Integrated Circuits in Si and GaAs*, Macmillan Publishing Company, New York
- [2] D. Kohler, B. Raabe, S. Braun, S. Seren, G. Hahn, "Upgraded metallurgical grade silicon solar cells: a detailed material analysis", Proc. 24<sup>th</sup> EU-PVSEC, Hamburg, 2009
- [3] S. Braun, B. Raabe, D. Kohler, S. Seren, G. Hahn, "Comparison of buried contact- and screen printed 100% UMG solar cells resulting in 16.2% efficiency", Proc. 24<sup>th</sup> EU-PVSEC, Hamburg, 2009
- [4] B. Raabe, K. Peter, E. Enabakk, G. Hahn, "Minority Carrier Lifetime Monitoring in a Buried Contact Solar Cell Process Using mc-Si", Proc. 23<sup>th</sup> EU-PVSEC, Valencia 2008
- [5] S. Hopmann, A. Fell, C. Fleischmann, K. Drew, D. Kray, F. Granek, "Study of laser parameters for silicon solar cells with LCP selective emitters", Proc. 24<sup>th</sup> EU-PVSEC, Hamburg, 2009
- [6] D.K. Schroeder, *Semiconductor Material and Device Characterization*, John Wiley & Sons INC., New York
- [7] G. Schubert, Dissertation, *Thick Film Metallisation of Crystalline Silicon Solar Cells: Mechanisms, Models and Applications*, University of Konstanz, 2006